07,05

$(Fe,Cr,Si)_{75}C_{25}$ Mechanosynthesised alloy: Mössbauer studies and magnetic hysteresis properties

© A.A. Chulkina, A.I. Ulyanov, A.L. Ulyanov

Federal State Budgetary Scientific Organisation Udmurt Federal Research Center
of Ural Branch of the Russian Academy of Sciences,
Izhevsk, Russia

E-mail: chulkina@udman.ru

Received May 29, 2025
Revised July 4, 2025
Accepted July 9, 2025

The magnetic properties of $(Fe_{1-x-y}Cr_xSi_y)_{75}C_{25}$ (where $x = 0.05$; 0.10, $y = 0.01$; 0.03) nanocrystalline alloys, obtained by mechanosynthesis and subsequent annealing, as well as the magnetic state of the phases in these alloys have been investigated using Mössbauer spectroscopy and magnetic measurements. The peculiarities of the magnetic hysteresis properties formation of these alloys were determined. It has been shown that the concentration of chromium atoms in cementite, emerging at crystallization of the X-ray amorphous phase, depends on the annealing temperature. After annealing at the temperatures of 500−600 °C the cementite fraction with maximum chromium content is formed in the alloys.

Keywords: mechanosynthesis, annealing, redistribution of alloying elements, Mössbauer spectroscopy, specific saturation magnetization, coercive force.

DOI: 10.61011/PSS.2025.08.62271.178-25

1. Introduction

Cementite plays an important role in forming mechanical characteristics of carbon steels. It is possible to control properties of steels and alloys by adjusting the cementite properties. In order to obtain optimal strength characteristics, the steels are alloyed, most often, by several alloying elements. The interest is paid to such alloying elements as chromium and silicon. Chromium increases corrosion resistance and toughness and increases stability of steel cementite. There are theoretical studies and experimental studies for investigating the properties of the chromium-alloyed cementite [1–8]. Incorporation of silicon into a composition of the steels contributes to improvement of their hardness, wear resistance and elasticity. What is especially interesting is a silicon capability of contributing to formation of fine-grained and, in some cases, nanoscale structures, too [9], in the steels, thereby significantly increasing the strength characteristics of silicon-containing steels. Formation of a nanostructure state is also affected by a method of producing such materials. The nanostructure state of the alloys, including those based on iron, is easily obtained by a method of mechanical synthesis (MS) of powders of initial elements in a ball planetary mill [10–13]. At this, the MS alloys are formed in a non-equilibrium state. Annealings make it possible to track kinetics of further phase formation and phase alloying in these alloys.

The present study continues investigating the properties of the $(Fe_{1-x-y}Cr_xSi_y)_{75}C_{25}$ mechanosynthesized alloys alloyed with the two elements (chromium and silicon), where $x = 0.05$; 0.10 and $y = 0.01$; 0.03, which are presented in the study [14]. The present study is aimed at investigating a magnetic state of the phases by Mössbauer spectroscopy, which is formed as a result of redistribution of the alloying elements during mechanosynthesis and subsequent annealings of the alloys. The obtained data will be taken to determine mechanisms of formation of magnetic hysteresis properties of the studied alloys. Besides, the Mössbauer studies will be used to discuss a hypothesis of the study [14] that an X-ray amorphous phase (XAP) of the $(Fe,Cr,Si)_{75}C_{25}$ alloys is crystallized in two stages, in which cementite fractions with a different chromium concentration are formed during annealings.

2. Samples and research methods

Purity of the initial components, production conditions, modes of thermal treatment of the studied samples of the $(Fe_{1-x-y}Cr_xSi_y)_{75}C_{25}$ mechanosynthesized alloys, where $x = 0.05$; 0.10 and $y = 0.01$; 0.03, are described in detail in the study [14].

The investigation methods used in the study [14] were supplemented by the Mössbauer studies in the present study. The Mössbauer spectra were measured in a spectrometer SM2201DR with a $^{57}Co(Rh)$ source in a transmission geometry in a constant acceleration mode both at the room temperature T_{room} and at the temperature of liquid nitrogen (−196 °C). An annealed carbonyl-iron powder was selected to be a standard absorber. The Mössbauer spectra were mathematically processed in a continuous representation by means of a Tikhonov generalized regularized algorithm for solving inverse incorrect problems [15] in order to restore the distribution function of hyperfine magnetic

fields $P(H)$. A sextet of Lorentz lines (a single-kernel model) was used as a kernel of the integral Fredholm equation. For this reason, along with components from the ferromagnetic systems in the fields $H > 40-50$ kOe, the functions $P(H)$ that are restored from spectra of the samples with a complex magnetic structure containing ferromagnetic and paramagnetic states, also have components with small ($0 \le H < 40-50$ kOe) values of the hyperfine magnetic fields H. Within the framework of the used model, these components correspond to paramagnetic doublets, but in reality for the paramagnetic components the hyperfine magnetic field shall be 0 kOe. In order to determine the iron content in the phases for these samples, we have additionally carried out discrete processing of the spectra by a least-square method using the Levenberg–Marquardt algorithm.

The magnetic characteristics of the samples were measured in a vibrating magnetometer with a maximum magnetizing field of 16 kOe.

For abbreviations, in a text of this article the $(Fe_{1-x-y}Cr_xSi_y)_{75}C_{25}$ alloys are referred to as CrxSiy, where $x = 0.05$; 0.10 and $y = 0.01$; 0.03.

3. Results and their discussion

The Mössbauer studies can confirm information specified in the study [14] about crystallization during annealings of the X-ray amorphous phase of the mechanosynthesized $(Fe,Cr,Si)_{75}C_{25}$ alloys in the two stages with formation of the cementite fractions with the different chromium concentration as well as obtain additional data. The Mössbauer spectra of the low-chromium alloys (Cr5Si1 and Cr5Si3) as well as the alloys with the increased content of chromium (Cr10Si1 and Cr10Si3) in the state after MS and annealings are shown in Figure 1, *a* and *b* and *c* and *d* (on the left) The functions $P(H)$ that are calculated by these spectra and reflect a density of probability of distribution of the hyperfine magnetic fields on nuclei of ^{57}Fe isotopes from atoms in the nearest neighborhood are shown in the same figures on the right. Phase components obtained as a result of discrete processing are shown above the spectra of the alloys Cr5Si3, Cr10Si1 and Cr10Si3 annealed at $T_{ann} = 600\,^{\circ}C$ (Figure 1, *b–d*). The study also included the same processing of the spectra of the alloys annealed up to $T_{ann} = 800\,^{\circ}C$ (it is not shown in the figures). The spectra of the alloys are measured at the temperature T_{room}.

A kind of the functions $P(H)$ of the main phases of the iron-carbon alloys is known. The functions $P(H)$ of the unalloyed cementite Fe_3C and α-Fe are single narrow peaks that correspond to average hyperfine magnetic fields on the nuclei of the iron isotopes $\langle H \rangle = 205$ kOe [16] and $\langle H \rangle = 330$ kOe [17]. In case of alloying these phases with chromium, the functions $P(H)$ are broadened, i. e. these functions exhibit additional components (peaks) at the side of the low magnetic fields H [7,18]. Appearance of the silicon atoms in the nearest neighborhood of the iron atoms in the ferrite (the solid solution of carbon and the alloying elements in α-Fe) similarly changes the function $P(H)$ of the unalloyed ferrite (α-Fe) [19]. The amorphous phase is characterized by a distribution of the function $P(H)$ in the wide range of the fields $H \approx (100-300)$ kOe [17].

Table 1. Probability W of the n Cr atoms in the nearest neighborhood of the Fe atoms in the cementite of the compositions $(Fe_{1-x}Cr_x)_3C$, where $x = 0.05$; 0.07; 0.10. The samples were annealed at 800 °C for 1 h [7]

n	W		
	$x = 0.05$	$x = 0.07$	$x = 0.10$
0	0.54	0.45	0.30
1	0.32	0.38	0.28
2	0.14	0.13	0.23
3	0	0.04	0.19
4	–	0	0

It follows from Figure 1, *a* and *b* (the curves *1* and *2*) that all the phases in the low-chromium alloys Cr5Si1 and Cr5Si3 both after MS and subsequent annealings up to $T_{ann} = 500\,^{\circ}C$ (until the first stage of XAP crystallization is finished, when carbides are released at the XAP portions with the minimum content of silicon) are in the ferromagnetic state. It is indicated by a distribution of the functions $P(H)$ within the wide interval of the magnetic fields $40-50 < H < 300$ kOe, which is typical for the X-ray amorphous phase and the alloyed carbide phases. The functions $P(H)$ of these phases overlap and it is impossible to isolate them separately. You can clearly see a free-standing peak of the function $P(H)$ in the field $\langle H \rangle = 330$ kOe, which is typical for α-Fe (or the unalloyed ferrite).

At the annealing temperatures $T_{ann} = (500-600)\,^{\circ}C$ the residual XAP in the alloys is now transformed in conditions of quite high mobility of the Cr and Si atoms; and at the same time the alloying elements are redistributed between the phases. These processes are most pronounced in the Cr5Si3 alloy (Figure 1, *b*, the curves *3* and *4*). The dependence $P(H)$ additionally exhibits a maximum in the field $\langle H \rangle = 25$ kOe. Within the framework of a single-kernel computation model, it describes a phase that is paramagnetic at T_{room}, which is a cementite fraction with the increase content of chromium [14]. Let us explain this fact. For the cementite with the different content of chromium $(Fe,Cr)_3C$, the study [7] has experimentally determined the probability of the Cr atoms in the first coordination sphere of the Fe atoms. This data is shown in Table 1.

Thus, at most three Cr atoms were detected with the maximum probability $W = 0.19$ in the nearest neighborhood of the Fe atoms in the cementite of the compositions $(Fe_{0.95}Cr_{0.05})_3C-(Fe_{0.90}Cr_{0.10})_3C$, whose Curie temperature decreased from 140 to 47 °C. The distribution functions $P(H)$ of the cementite of these compositions

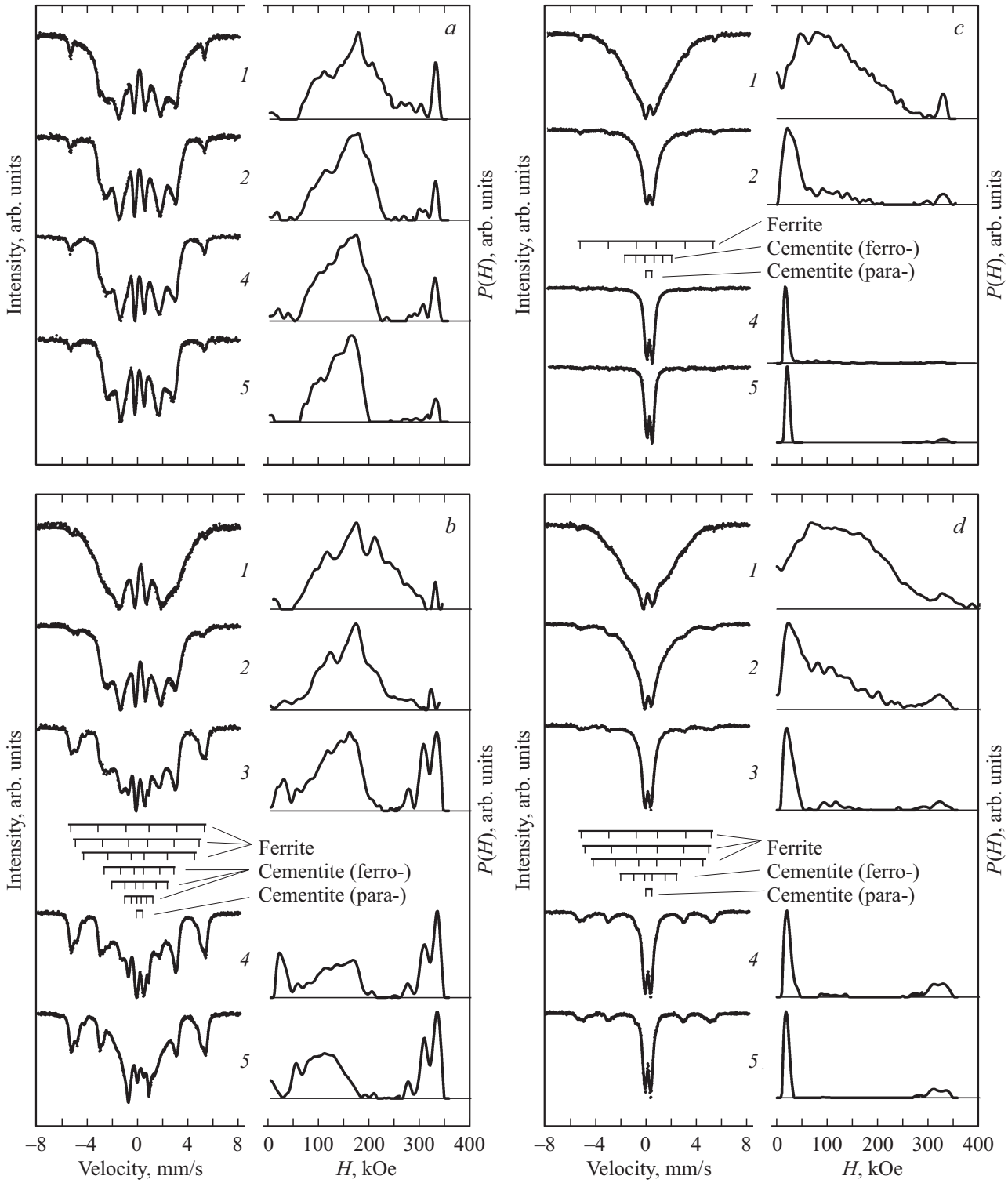

Figure 1. Mössbauer spectra (on the left) and their respective functions $P(H)$ (on the right) of the alloys: *a*) Cr5Si1; *b*) Cr5Si3; *c*) Cr10Si1; *d*) Cr10Si3 in the state after: *1* — MS and annealing at the temperature T_{ann}: *2* — 500, *3* — 550, *4* — 600, *5* — 800. The measurement temperature T is the room temperature T_{room}.

were in the fields $50 \leq H \leq 205$ kOe and reflected the ferromagnetic state of the phase. With further increase of the concentration of the chromium atoms in the cementite composition, the number of the Fe atoms, whose nearest neighborhood includes a small number of the chromium atoms, will be decreased. Consequently, the number of the Fe atoms with the first coordination sphere's population of at least three atoms of this alloying element will be

increased. For example, it can be assumed that after annealing $T_{ann} > 500\,^{\circ}C$ the Cr5Si3 alloy at T_{room} has varieties (fractions) of the cementite, which differ by the Cr concentration — ferromagnetic and paramagnetic. By extrapolating the dependence $T_C(x)$ of the $(Fe_{1-x}Cr_x)_{75}C_{25}$ alloy, it was found by the data of the study [7] that the cementite with the Curie temperature $T_C = 25\,^{\circ}C$ shall have had the composition $(Fe_{0.89}Cr_{0.11})_3C$. We have performed a similar procedure of extrapolation, and based on the data of Table 1 built the dependences $W(x)$ for the different amount n of the Cr atoms in the nearest neighborhood of the Fe atoms. It was obtained that in the $(Fe_{0.89}Cr_{0.11})_3C$ cementite the probability of the three Cr atoms in the nearest neighborhood of the Fe atoms was $W \approx 0.25$. It follows that if the probability of the three Cr atoms in the nearest neighborhood of the Fe atoms will be $W > 0.25$ or the fourth Cr atom will appear in the nearest neighborhood of the Fe atoms, then this cementite will be in the paramagnetic state and have a doublet component in the Mössbauer spectrum.

As follows from a graph of the dependences of the phase composition on T_{ann}, which is shown in the study [14] in Figure 2 (the curves *3*), annealing of the alloys Cr5Si3 and Cr10Si3 at $T_{ann} = (500-600)\,^{\circ}C$ results in precipitation of a large amount of ferrite alloyed with silicon, which previously (at the smallerT_{ann}) prevented release of carbide phases from the XAP. In Figure 1, *b*, the curves *3* and *4* (on the right), alloying of ferrite of the Cr5Si3 alloy can be judged by appearance of intense peaks of the function $P(H)$ with the average magnetic fields $\langle H \rangle = 331$, 305 and 273 kOe. By comparing the obtained form of distribution of $P(H)$ with literature data [18,19], it can be concluded that the nearest neighborhood of the Fe atoms has, respectively, 0, 1 or 2 atoms of the alloying elements — both of silicon and, possibly, of chromium. It should be noted that although chromium in the iron-carbon chromium alloy is mainly in cementite, a certain number of atoms of this element is dissolved in ferrite, too [20]. It is difficult to separate contributions by the atoms Cr and Si in the nearest neighborhood of the Fe atoms, since they approximately equally affect variation of the hyperfine magnetic field of pure α-Fe. After annealing at $T_{ann} = 600\,^{\circ}C$ the Cr5Si3 alloy transits into the two-phase state — it consists of ferrite alloyed with Si and Cr and cementite, whose fractions have the different concentration of the Cr atoms and, therefore, the different Curie temperature. Further increase of T_{ann} up to $800\,^{\circ}C$ reduces inhomogeneity of distribution of the chromium atoms in cementite (Figure 1, *b* — the curve *5*, on the right), but does not eliminate it completely.

The similar processes of crystallization of the residual XAP occur in the Cr5Si1 low-chromium alloy as well. Due to a small amount of silicon in the alloy after completion of the first stage of crystallization ($T_{ann} = 500\,^{\circ}C$), a volume of the residual XAP alloyed with this element is small. It is difficult to correctly distinguish such an amount of the phase from X-ray patterns. Therefore, we will assume that the Cr5Si1 alloy also transits into the two-phase state

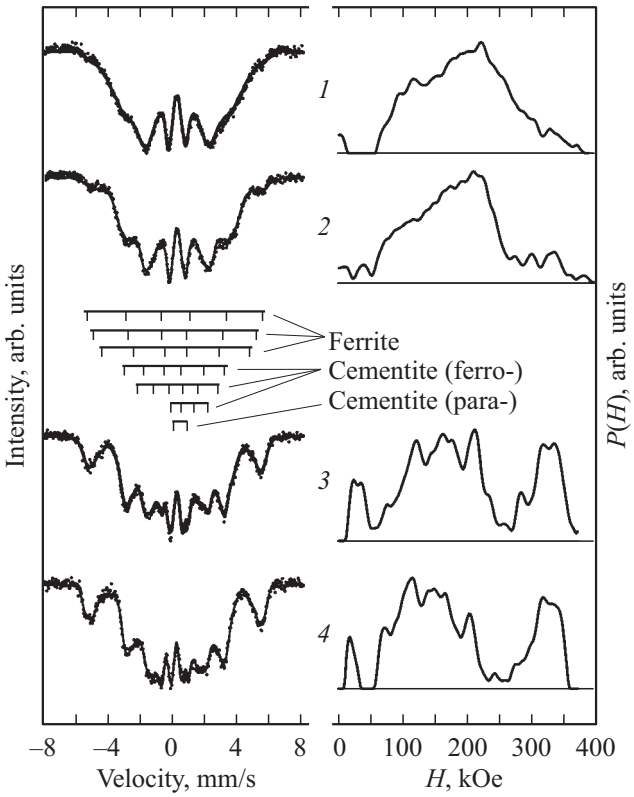

Figure 2. Mössbauer spectra (on the left) and their respective functions $P(H)$ (on the right) of the Cr10Si3 alloy after: *1* — MS and annealing at the temperatures T_{ann}: *2* — 500, *3* — 600, *4* — 800 °C. The measurement temperature is $T = -196\,^{\circ}C$.

within the interval $500 < T_{ann} \leq 600\,^{\circ}C$. All the phases of this alloy are in the ferromagnetic state irrespective of the annealing temperature. It is indicated by a distribution of the function $P(H)$ of the alloy in the hyperfine magnetic fields $H > 50$ kOe (Figure 1, *a*). The functions $P(H)$ of ferrite and ferromagnetic cementite of this two-phase alloy do not overlap, and therefore, it is possible to determine a portion S of the Fe atoms contained in each phase by relative areas under curves of the functions $P(H)$ of these phases. Table 2 presents results of these calculations.

After MS, the alloys with the increased content of chromium (Cr10Si1 and Cr10Si3) contain not only a large volume of the ferromagnetic phases — XAP, carbides and ferrite ($H > 40-50$ kOe), but also a certain amount of the paramagnetic phases — paramagnetic carbides (according to the single-kernel model of processing $H < 40-50$ kOe). This statement follows from analysis of the functions $P(H)$ that are restored from the Mössbauer spectra measured at T_{room} (Figure 1, *c* and *d*, the curves *1*) as well as from X-ray diffraction analysis data (Figure 2, *b* and Table 2 in the study [14]). With increase of T_{ann} the content of the paramagnetic carbides only increases (Figure 1, *c* and *d*, the curves *2*–*5*). After annealing at $600\,^{\circ}C$ the alloys are in the two-phase state, i. e. they consist of ferrite and cementite, whose fractions have the different concentration

Table 2. Interval of the hyperfine magnetic fields H of distribution of the function $P(H)$ of the phases (ferrite and ferromagnetic cementite) and the portion S of the Fe atoms in the phases as applied to the annealed $(Fe_{1-x-y}Cr_xSi_y)_{75}C_{25}$ alloys that are in the two-phase state. The Mössbauer spectra were measured: at the temperature $T = T_{room}$ (the unbracketed data) and when $T = -196\,^{\circ}C$ (the bracketed data)

T_{ann}, °C	Phases				
	α-Fe		Ferromagnetic cementite		Paramagnetic cementite
	H, kOe	S, %	H, kOe	S, %	S, %
Cr5Si1 alloy					
600	270–350	10	50–225	90	–
800	260–350	8	50–200	92	–
Cr5Si3 alloy					
600	255–350 (270–350)	39 (40)	45–210 (50–250)	45 (60)	16 (–)
800	250–350	40	25–200	57	3
Cr10Si1 alloy					
600	280–350 (280–350)	3 (3)	40–120 (40–290)	14 (97)	83 (–)
800	250–350 (250–375)	8 (10)	– (50–250)	– (90)	92 (–)
Cr10Si3 alloy					
600	265–349 (270–370)	31 (27)	84–144 (50–240)	3 (65)	66 (8)
800	250–350 (260–360)	31 (27)	– (50–240)	– (69)	69 (4)

of the Cr atoms. For these alloys, the portion S of the Fe atoms contained in each phase was determined by discrete processing (Table 2).

It follows from Table 2 that at T_{room} after annealing at 800 °C cementite in the low-chromium alloys either can be only in the ferromagnetic state as in the Cr5Si1 alloy or can have paramagnetic fractions as in the Cr5Si3 alloy. After similar thermal treatment, in the alloys with the increased content of chromium all of cementite is in the paramagnetic state.

Since the alloys with the increased content of chromium mainly consist of the paramagnetic phases, it is interesting to study the Mössbauer spectra of the alloys, which are taken at the temperature below the Curie point of their main phases. The Mössbauer spectra of the alloys Cr10Si1 and Cr10Si3 were measured at the temperature of liquid nitrogen $T = -196\,^{\circ}C$. The $P(H)$ functions were analyzed to show that after MS and subsequent annealings all the phases of the Cr10Si1 alloy become ferromagnetic. The article does not provide spectra of these alloy, but Table 2 includes portions of the Fe atoms distributed between ferromagnetic cementite and ferrite after annealings at $T_{ann} = 600$ and 800 °C. Another situation is observed for the Cr10Si3 alloy, whose spectra and functions $P(H)$ are shown in Figure 2. It is clear that after MS (the curve *1*) and annealings at up to 500 °C (the curve *2*) all the phases of this alloy are ferromagnetic, while their overlapping functions $P(H)$ are in the range of the fields H from 60 to 380 kOe. The situation changes during the second stage of XAP crystallization at $T_{ann} = 500–600\,^{\circ}C$ (the curve *3*). First of all, a significant amount of alloyed ferrite is released in the Cr10Si3 alloy similar to the Cr5Si3 low-chromium alloy (Figure 2, *a* and *b*, the curve *3* of the study [14]). The function $P(H)$ of ferrite of the Cr10Si3 alloy is within the range of the fields $H = (270–370)$ kOe (Figure 2, the curve *3*; Table 2). Secondly, the Curie temperature of cementite formed from the residual XAP turned out to be below the temperature of liquid nitrogen, i.e. this cement is paramagnetic when $T = -196\,^{\circ}C$. The Mössbauer spectrum of this sample has a doublet, while the function $P(H)$ includes a component when $H < 50$ kOe (Figure 2, the curve *3*). The Mössbauer spectra of this alloy annealed when $T_{ann} \geq 600\,^{\circ}C$ were processed in a discrete representation. Figure 2 (as an example) shows decomposition of the spectrum of the alloy annealed when $T_{ann} = 600\,^{\circ}C$ into phase components, while the results of the calculations are given in Table 2. Thus, in the Cr10Si3 alloy, cementite annealed at $T_{ann} = 600\,^{\circ}C$ (at the measurement temperature $T = -196\,^{\circ}C$) consists of a paramagnetic and a ferromagnetic part (fraction). These fractions include, respectively, 8 and 65% of the Fe atoms contained in the alloy. The ferromagnetic part of such a cementite is formed during MS and as a result of the first stage of XAP crystallization (distribution of the function $P(H)$ within the range of the magnetic fields $H = 50–240$ kOe, Figure 2, the curve *3*; Table 2). The remaining Fe atoms are in ferrite. A similar situation was observed in the Cr5Si3 alloy annealed when $T_{ann} \geq 600\,^{\circ}C$, but at the room temperature of measurement of the Mössbauer spectra. With increase of the annealing temperature of the Cr10Si3 alloy, the portion of paramagnetic cementite is reduced. However, even after annealing at 800 °C this alloy has local areas of cementite, whose T_C is below the temperature of liquid nitrogen (Figure 2, the curve *4*; Table 2). Up to 4% of all the Fe atoms in the alloy is contained in these areas (Table 2). Based on the foregoing, it can be concluded that variation of an atomic composition of the studied alloys and modes of their thermal treatment results in variety of the magnetic states of the phased contained therein, which shall inevitably affect the magnetic properties of these alloys.

The magnetic state of the phases determines a value of specific saturation magnetization σ_s of the studied alloys. The structural state of the phases and their interaction during magnetization and remagnetization affect the magnetic hysteresis properties of the studied materials, in particular, a value of their coercive force H_c. Figure 3

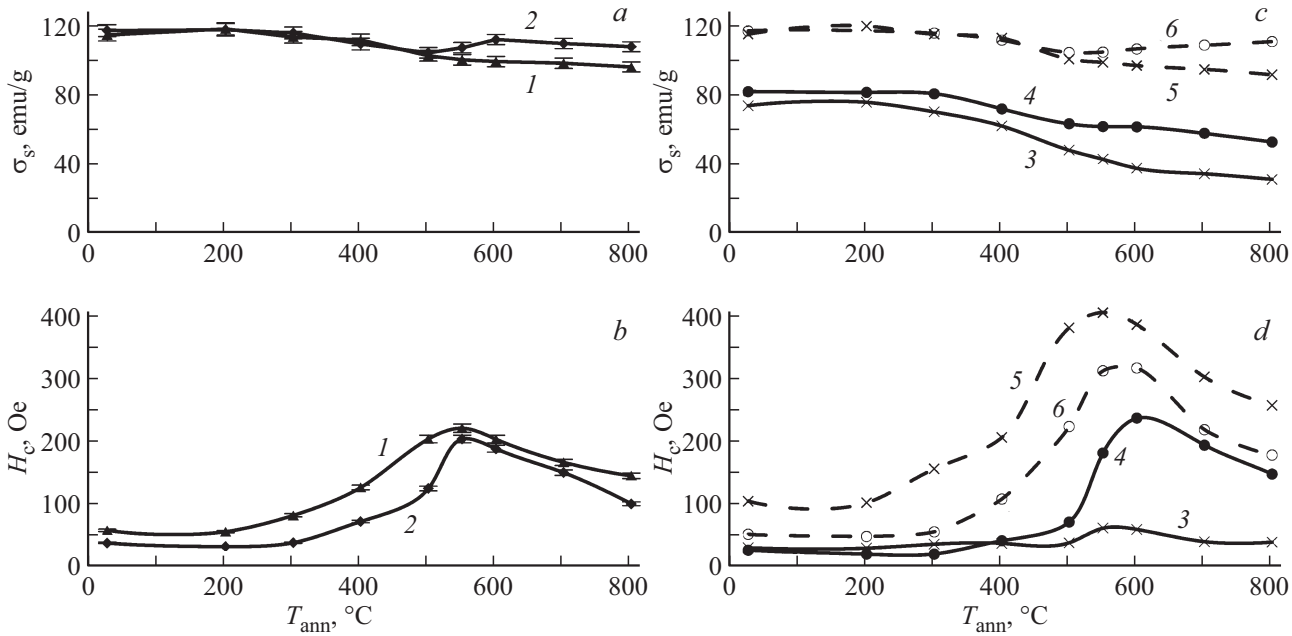

Figure 3. Dependence on the annealing temperature T_{ann}: *a* and *c* — for specific saturation magnetization σ_s; *b* and *d* — for the coercive force H_c of the alloys: *1* — Cr5Si1; *2* — Cr5Si3; *3, 5* — Cr10Si1; *4, 6* — Cr10Si3. The measurement temperature *T*: *1–4* — T_{room}; *5* and *6* — (−196) °C.

shows the dependences of specific saturation magnetization σ_s and the coercive force H_c of the discussed alloys on the annealing temperature. It is clear that in the state after MS the values of σ_s of the low-chromium alloys, which are measured at T_{room}, are $\sim 115-117$ emu/g (Figure 3, *a*). The dependences $\sigma_s(T_{ann})$ of the low-chromium alloys Cr5Si1 and Cr5Si3 are almost the same up to $T_{ann} = 500\,^{\circ}C$ inclusively. By comparing the phase composition within the interval $T_{ann} < 500\,^{\circ}C$ [14], it can be assumed that the values of σ_s of cementite, χ-carbide and XAP of these alloys are close to each other. The situation changes with a start of the second stage of crystallization of the residual XAP ($T_{ann} > 500\,^{\circ}C$), when mobility of the atoms in the alloys starts increasing. Thus, unlike Cr5Si1 (Table 2 [14]), the content of ferrite significantly increases in the Cr5Si3 alloy (Figure 2, *a*, the curve *3* [14]), thereby resulting in the increase of specific saturation magnetization σ_s of this alloy within the interval $T_{ann} = 500-600\,^{\circ}C$. Further increase of T_{ann} slightly affects variation of σ_s of the low-chromium alloys.

After MS, specific saturation magnetization of the high-chromium alloys, which is measured at T_{room}, has the values $\sigma_s \approx 75-82$ emu/g (Figure 3, *c*, the curves *3* and *4*), which is significantly lower than σ_s of the low-chromium alloys. One of the causes of it is the fact that the chromium atoms have antiferromagnetic ordering with the iron atoms. This circumstance results in reduction of the magnetic moments of those iron atoms, which have the chromium atoms as the nearest neighbors. Based on this, the values of σ_s of the phases that contain iron and chromium atoms will also be reduced [6]. Thus, as the Cr concentration in cementite increases, its specific saturation magnetization σ_s will decrease. In particular, at the room temperature of measurement σ_s of cementite in the high-chromium alloys can decrease up to zero values. As follows from the curves *1* in Figure 1, *c* and *d*, after MS the alloys Fe10Si1 and Fe10Si3 already have paramagnetic fractions of cementite. With increase of the annealing temperature, a volume of the paramagnetic fractions only increases, thereby determining intense reduction of σ_s of the Cr10Si1 alloy within the interval T_{ann} from 400 to 600 °C (the curve *3* in Figure 3, *c*). The value of specific saturation magnetization of the Cr10Si3 alloy is almost unchanged within the interval $T_{ann} = 500-600\,^{\circ}C$ due to effect of two opposite factors: 1 — reduction of σ_s of cementite due to transition of a part of its volume from the ferromagnetic to paramagnetic state; 2 — increase of σ_s due to increase of the volume of ferrite during the second stage of XAP crystallization.

Figure 3, *c* also shows dependences $\sigma_s(T_{ann})$ of the high-chromium alloys, which are measured at the temperature of liquid nitrogen. At the same time, the phases (or the phase fractions) that are paramagnetic at the room temperature of the measurements transit into the ferromagnetic state, thereby increasing the value of σ_s of the alloys (the curves *5* and *6*). However, a nature of the dependences $\sigma_s(T_{ann})$ is still almost the same as it was at the room temperature of the measurements.

Changes of the structure-phase state, which occur during annealings of the MS alloys, visualize the dependences $H_c(T_{ann})$ shown in Figure 3, *b* and *d*. It is clear that these dependences have a non-monotonic nature. After MS, the alloys have a relatively low value $H_c \approx 20-45$ A/cm,

whose formation is affected by magnetic properties of a mixture of the phases: XAP, carbides with distorted crystal lattices and ferrite. In particular, a nanocrystalline cementite with a strongly distorted crystal lattice is formed during MS [13]. Carbon atoms in the distorted lattice of cementite are predominantly arranged not in prismatic (as usual), but octahedral sites. This circumstance significantly (by an order of magnitude) reduces [21] a magnetocrystalline anisotropy constant K and, therefore, H_c of cementite as compared to H_c of cementite with an undistorted lattice.

Let us consider the influence of annealings on variation of H_c of the low-chromium alloys (Figure 3, *b*). It is clear that after annealings when $T_{ann} > 200\,^{\circ}C$ H_c of the Cr5Si1 alloy starts increasing (the curve *1*), which is primarily related to gradual release of distortions of the crystal lattice of cementite and the transition of the carbon atoms into the prismatic sites. It results in increase of the magnetocrystalline anisotropy constant K of cementite and, therefore, in increase of its H_c. Annealing at the temperature of $550\,^{\circ}C$ generally releases distortions of the lattices, thereby almost entirely restoring the constant K of cementite. After such thermal treatment, the coercive force of the alloy, namely, the maximum value $H_c = 176$ A/cm in the dependence $H_c(T_{ann})$ will be predominantly determined by coercivity of ferromagnetic cementite alloyed with chromium [7], since its content in the Cr5Si1 alloy is ~ 94 vol.%, while the remaining part is ferrite (Table 2 of the study [14]). During annealings at $T_{ann} > 600\,^{\circ}C$, a density of defects of the crystal structure starts intensely decreasing in the phases of the Cr5Si1 alloy, including in cementite, thereby resulting in reduction of H_c of the alloy (Figure 3, *b*, the curve *1*).

Formation of the carbide at annealings at up to $500\,^{\circ}C$ is hindered in the Cr5Si3 alloy with the increased content of silicon due to the fact that the Si atoms prevent a growth of the carbide phases, in particular, cementite, inhibiting arrival of the carbon atoms to them [22–25]. As compared to the Cr5Si1 alloy that after annealing at $500\,^{\circ}C$ mainly consists of cementite (Table 2 of the study [14]), the Cr5Si3 alloy after similar thermal treatment includes only 27 vol.% of cementite (Figure 2, *a*, the curve *2* of the study [14]). A small amount of high-coercivity cementite determines a lower value of H_c of the Cr5Si3 multi-phase alloy as compared to H_c of the Cr5Si1 alloy (Figure 3, *b*). The situation changes after annealings when $T_{ann} > 500\,^{\circ}C$, when the Si atoms obtain high mobility. They alloy ferrite that is released from the residual XAP. Simultaneously with precipitation of ferrite, in addition to MS cementite and cementite formed as a result of the first stage of XAP crystallization, cementite with the increased concentration of chromium is formed [14]. But according to the Mössbauer spectra (Figure 1, *b*, the curves *3* and *4*), the areas of cementite with the increased Cr concentration are paramagnetic at the room temperature (Table 2). They act as nonmagnetic inclusions (pores) during remagnetization of the ferromagnetic matrix that consists of ferrite and cementite formed during MS and the first stage of XAP crystallization. Therefore, sharp increase of H_c of the Cr5Si3 alloy with increase of the annealing temperature within the interval $500-550\,^{\circ}C$ is caused by joint effect of pinning of domain walls on the nonmagnetic inclusions and a growth of the magnetocrystalline anisotropy constant of ferromagnetic cementite. Annealing at $800\,^{\circ}C$ results in more uniform distribution of chromium in cementite. After such annealing, the content of paramagnetic cementite in the alloy greatly decreases (Figure 1, *b*, the curve *5*; Table 2). A contribution to H_c by pinning of the domain walls on the nonmagnetic inclusions almost disappears. In this regard, reduction of H_c within the interval $T_{ann} = 700-800\,^{\circ}C$ for the Cr5Si3 alloy is much faster than for the Cr5Si1 alloy that had no nonferromagnetic inclusions after annealings within the entire studied temperature interval.

Figure 3, *d* shows dependences $H_c(T_{ann})$ of the alloys Cr10Si1 and Cr10Si3 with the increased content of chromium (the curves *3* and *4*), which are measured at T_{room}. Unlike the low-chromium alloys, the phases of these alloys after MS are more strongly alloyed with chromium, thereby resulting in reduction of the value of their H_c to 20 A/cm. During further annealings up to the temperature $400-500\,^{\circ}C$ similar processes occur in the alloys Cr10Si1 and Cr10Si3: the distortions of the lattices of the carbide phases are released with restoration of their constant K and the phase transformations occur. The values of their H_c are close. However, after annealing when $T_{ann} = 550\,^{\circ}C$ the coercive force H_c of the Cr10Si3 alloy sharply increases, reaching a maximum value when $T_{ann} = 600\,^{\circ}C$, and after that it decreases with further increase of the annealing temperature. As compared to H_c of the Cr10Si3 alloy, the coercive force of the Cr10Si1 alloy after annealing within this temperature interval slightly changes. Let us discuss causes that result in a substantial difference at the room temperature of the measurements in the values of H_c of these alloys annealed at the temperatures $T_{ann} \geq 550-600\,^{\circ}C$. After annealing when $T_{ann} = 600\,^{\circ}C$, as follows from Table 2, the alloys are nonferromagnetic matrices that consist of paramagnetic cementite with ferromagnetic inclusions distributed therein. In the Cr10Si1 alloy, the inclusions are mainly presented by ferromagnetic cementite, in which up to 14 at.% Fe (of its entire amount in the alloy) and ferrite (up to 3 at.% Fe) are contained according to the Mössbauer data (Table 2).

The reverse ratio is observed in the Cr10Si3 alloy: ~ 31 and 3% of the Fe atoms are respectively in the inclusions of ferrite and ferromagnetic cementite. It can be concluded based on the provided data that the coercive force of the Cr10Si1 alloy annealed at the temperatures $550-700\,^{\circ}C$ is mainly determined by coercivity of ferromagnetic cementite. The low values of its H_c are due to quite high alloying of cementite with chromium [7]. The coercive force is formed in the Cr10Si3 alloy in a fundamentally different mechanism, namely, by remagnetization of ferrite precipitations that are in paramagnetic cementite and whose size is close to a single-domain state. It is known [26] that Fe particles that have a critical single-domain size and are magnetically isolated from each other by paramagnetic

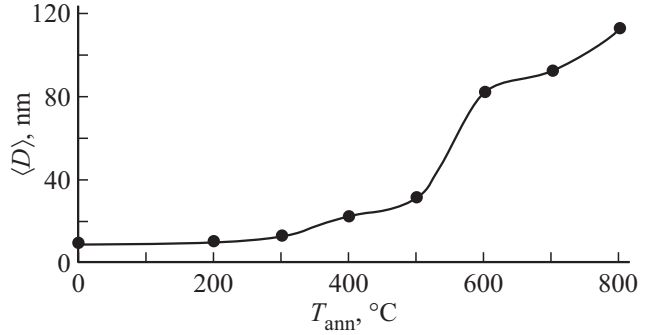

Figure 4. Average size $\langle D \rangle$ of coherent scattering blocks of α-Fe in the Cr10Si3 alloy in a dependence on the annealing temperature T_{ann}.

phase interlayers are remagnetized during measurement of the coercive force by coherent rotation of magnetization in fields that are close to a field of magnetocrystalline anisotropy of matter. According to the study [27], the coercive force of the single-domain Fe particles with the critical size $d_0 = 21$ nm can be up to $H_c \approx 1210$ Oe. As the size increases, the coercive force of the particles decreases, since even with the absence of the domain walls in the particle the inhomogeneous distribution of magnetization mainly of a vortex type starts to form. With further increase of the size, the particles gradually transit from the single-domain state into the multi-domain state, thereby causing subsequent reduction of their H_c [28]. Thus, the coercive force of bulk samples made of technically pure cast iron can be up to $H_c \approx 0.9$ Oe [29].

Figure 4 shows a dependence of the average size of the coherent scattering areas of ferrite in the Cr10Si3 alloy on the annealing temperature. For the nanomaterials, it is close to an average size $\langle D \rangle$ of grains of the ferrite phase. It is clear that $\langle D \rangle$ of the ferrite grains are really within a nanometer range. Thus, the Cr10Si3 alloy after annealing at 600 °C can be represented as a paramagnetic cementite matrix, which includes mainly precipitations of the ferrite phase with the average size of $\langle D \rangle \approx 80$ nm (Figure 4). This size of the ferrite grains is much larger than the critical single-domain size of the Fe particles. Therefore, the expected value of H_c of the alloy shall be below 1210 Oe, which is experimentally observed. After annealing the Cr10Si3 alloy at 600 °C $H_c^{max} \approx 240$ Oe (Figure 3, *d*, the curve *4*). With further increase of T_{ann}, the average grain size increase, while H_c of the alloy decreases respectively.

Reduction of the measurement temperature to −196 °C results in a change of the values of the coercive force of the alloys. Figure 3, *d* (the curves *5* and *6*) shows dependences $H_c(T_{ann})$ of the alloys with the increased content of chromium, which are measured at the temperature of liquid nitrogen. It is clear that H_c of the alloys at all the values of T_{ann} significantly increase, which is due to several reasons. First of all, as the measurement temperature decreases, the magnetocrystalline anisotropy constant of cementite increases [30], thereby resulting in increase of its H_c [31]. Secondly, at the temperature of liquid nitrogen all of cementite of the Cr10Si1 alloy and a significant amount of cementite of the Cr10Si3 alloy become ferromagnetic. Thus, after annealing at 600 °C the Cr10Si1 alloy has only ferromagnetic phases — Si- and Cr-alloyed ferrite (Table 2, $S = 3\%$) and Cr-alloyed cementite (Table 2, $S = 97\%$); and the coercive force of the latter generally determines the maximum $H_c^{max} \approx 410$ Oe of this alloy.

The Cr10Si3 alloy after annealing at 600 °C has ferrite ($S = 27\%$) and paramagnetic ($S = 8\%$) and ferromagnetic ($S = 65\%$) cementites (Table 2). It follows from the provided data that ferrite precipitations are now surrounded by ferromagnetic cementite. Consequently, when the coercive force is measured, the ferrite precipitations turn into a normal soft magnetic phase. Thus, a decisive role in forming the maximum value $H_c^{max} \approx 330$ Oe of the Cr10Si3 alloy is also played by coercivity of ferromagnetic cementite. The lower value of H_c^{max} of this alloy as compared to H_c^{max} of the Cr10Si1 alloy is caused, first of all, by a higher content of the soft magnetic phase therein (Table 2). Secondly, cementite of the Cr10Si3 alloy is alloyed with chromium in a higher degree than the Cr10Si1 alloy (Figure 6, *b* and *d*, the curve *6* of the study [14]), thereby also reducing H_c of cementite and, therefore, of the alloy as well.

Taking into account the atomic composition, data of X-ray diffraction analysis and the Mössbauer studies about the magnetic state of the alloy phases, it can be concluded that the mechanisms for reversing magnetization of the alloys Cr10Si1 and Cr10S3 at the nitrogen measurement temperature will be similar to the mechanisms of remagnetization of the alloys Cr5Si1 and Cr5Si3, respectively, which are measured at T_{room}. If so, a nature of their dependences $H_c(T_{ann})$ shall be similar, too, which is really seen from comparing the curves *1* and *2* in Figure 3, *b* and the curves *5* and *6* in Figure 3, *d*, respectively.

4. Conclusions

1. The Mössbauer measurements and the magnetic measurements at the room temperature and the temperature of −196 °C were taken to study the magnetic state of the phases as well as the magnetic properties of the $(Fe_{1-x-y}Cr_xSi_y)_{75}C_{25}$ alloys, where $x = 0.05$; 0.10, and $y = 0.01$; 0.03, after mechanosynthesis (MS) and subsequent annealings up to the temperature of 800 °C. It is found that at the room measurement temperature all the phases of the Cr5Si1 alloy are in the ferromagnetic state irrespective of the annealing temperature, while the phases of the Cr5Si3 alloy are ferromagnetic only after annealing to $T_{ann} = 500$ °C. After annealing when $T_{ann} > 500$ °C, a certain part of cementite of this alloy becomes paramagnetic, forming the inclusions (pores) in the ferromagnetic matrix. Both after MS and after annealings, the alloys Cr10Si1 and Cr10Si3 have both ferromagnetic as well as paramagnetic phases. After annealing at 600 °C the alloys

with the increased content of chromium are a paramagnetic cementite matrix that has the ferromagnetic inclusions. In the Cr10Si1 alloy, the inclusions are mainly presented by ferromagnetic cementite, while in the Cr10Si3 they are mainly presented by ferrite. At the temperature of liquid nitrogen all the phases of the alloys (except for Cr10Si3) become ferromagnetic. After annealing the Cr10Si3 alloy when $T_{ann} > 500\,^{\circ}C$, a certain amount of paramagnetic cementite is detected.

2. It is found that for all the studied alloys the dependences of the coercive force H_c on the annealing temperature, which are measured both at T_{room} and at the temperature of liquid nitrogen, are curves with a maximum at the temperatures $T_{ann} = 550-600\,^{\circ}C$. The causes of formation of these maximums at the said measurement temperatures are different. Except for the Cr10Si3 alloy measured at the room temperature, the increase of H_c in line with an increase of T_{ann} of the studied alloys is mainly related to the magnetocrystalline anisotropy constant of alloyed cementite, which changes its structural state during annealings. Further increase of T_{ann} intensely remove defects of the crystal structure of the phases, especially, cementite, thereby resulting in reduction both of their H_c and H_c of the alloys. For the Cr10Si3 alloy, at T_{room}, the maximum values of H_c in the dependence $H_c(T_{ann})$ are generally formed due to remagnetization of ferrite particles that are close to the single-domain size and contained in the paramagnetic matrix.

3. The Mössbauer studies were taken to confirm the two stages in the process of crystallization (during annealings) of the X-ray amorphous phase of the $(Fe,Cr,Si)_{75}C_{25}$ mechanosynthesized alloys with formation of the cementite fractions with the different chromium concentration. The first stage of XAP crystallization occurs within the interval of the annealing temperatures $300-500\,^{\circ}C$ and is characterized by precipitation of carbides with a chromium concentration that is pre-defined by the initial composition. The second stage of crystallization of the residual XAP occurs within the narrow interval of the annealing temperatures $500-600\,^{\circ}C$, when the atoms of the alloying elements obtain quite high mobility. Cementite that is formed at this stage of crystallization has the increased Cr concentration, i. e. higher than the concentration pre-defined by the initial composition of the alloy. With increase of the annealing temperature, inhomogeneity of distribution of chromium in cementite is reduced, but even after one-hour annealing when $T_{ann} = 800\,^{\circ}C$ it is still high.

Funding

The study was carried out using the equipment of the Shared Use Center „Center of Physical and Physicochemical Methods of Analysis and Study of Properties and Characteristics of the Surface, Nanostructures, Materials and Products“ of the Udmurt Federal Research Center of the Ural Branch of RAS within the framework of the state assignment of the Ministry of Science and Higher Education of the Russian Federation (No. of state registration 124021900079-9).

Conflict of interest

The authors declare that they have no conflict of interest.

References

[1] T. Shigematsu. J. Phys. Soc. Japan **39**, *4*, 915 (1975).
[2] P. Schaaf, S. Wiesen, U. Gonser. Acta Metall. Mater. **40**, *2*, 373 (1992). https://doi.org/10.1016/0956-7151(92)90311-2
[3] M. Umemoto, Z.G. Liu, K. Masuyama, K. Tsuchiya. Scripta Materialia **45**, *4*, 391 (2001). https://doi.org/10.1016/S1359-6462(01)01016-8
[4] F.-Q. Zhao, O. Tegus, B. Fuquan, E. Bruck. J. Minerals, Metallurgy. Mater. **16**, *3*, 314 (2009). http://dx.doi.org/10.1016/S1674-4799(09)60056-X
[5] Z.Q. Lv, W.T. Fu, S.H. Sun, X.H. Bai, Y. Gao, Z.H. Wang, P. Jiang. JMMM **323**, *7*, 915 (2011). https://doi.org/10.1016/j.jmmm.2010.11.067
[6] M.A. Konyaeva, N.I. Medvedeva. Phys. Solid State **51**, *10*, 2084 (2009).
[7] A.A. Chulkina, A.I. Ulyanov, A.L. Ulyanov, I.A. Baranova, A.V. Zagainov, E.P. Yelsukov. Phys. Metals. Metallogr. **116**, *1*, 19 (2015).
[8] H.K.D.H. Bhadeshia. Int. Mater. Rev. **65**, *1*, 1 (2020). https://doi.org/10.1080/09506608.2018.1560984
[9] E. Houdremont. Handbuch der Sonderstahlkunde. Springer Verlag, Berlin (1956).
[10] A.I. Gusev. Nanomaterialy, nanostruktury, nanotekhnologii. Fizmatlit, M. (2009). 416 s. (in Russian).
[11] C. Suryanarayana, N. Al-Aqeeli. Progr. Mater. Sci. **58**, *4*, 383 (2013). https://doi.org/10.1016/j.pmatsci.2012.10.001
[12] Y.Z. Chen, A. Herz, Y.J. Li, C. Borchers, P. Choi, D. Raabe, R. Kirchheim. Acta Materialia **61**, *9*, 3172 (2013). https://doi.org/10.1016/j.actamat.2013.02.006
[13] E.P. Yelsukov, G.A. Dorofeev, V.M. Fomin, G.N. Konygin, A.V. Zagainov, A.N. Maratkanova. Phys. Metals. Metallogr. **94**, *4*, 356 (2002).
[14] A.A. Chulkina, A.I. Ulyanov. FTT **67**, *3*, 528 (2025). (in Russian).
[15] E.V. Voronina, N.V. Ershov, A.L. Ageev, Yu.A. Babanov. Physica Status Solidi (b) **160**, *2*, 625 (1990). https://doi.org/10.1002/pssb.2221600223
[16] E.P. Elsukov. A.L. Ul'yanov, D.A. Vytovtov. Bull. RAS: Phys. **71**, *9*, 1249 (2007).
[17] E.P. Yelsukov, G.A. Dorofeev, A.V. Zagainov, N.F. Vildanova, A.N. Maratkanova. Mater. Sci. Eng. A **369**, *1–2*, 16 (2004). https://doi.org/10.1016/j.msea.2003.08.054
[18] Yu.V. Baldokhin, V.V. Cherdyntsev. Inorg. Mater. **54**, *6*, 537 (2018). https://doi.org/10.1134/S0020168518060018
[19] A.F. Lehlooh, S.M. Fayyad, S.H. Mahmood. Hyperfine Interactions **139**, *1*, 335 (2002). https://doi.org/10.1023/A:1021237804221
[20] C.K. Ande, M.H.F. Sluiter. Acta Materialia **58**, *19*, 6276 (2010). https://doi.org/10.1016/j.actamat.2010.07.049
[21] A.K. Arzhnikov, L.V. Dobysheva, C. Demmangeat. J. Phys.: Condens. Matter. **19**, *19*, 196214 (2007). https://doi.org/10.1088/0953-8984/19/19/196214

[22] G. Miyamoto, J. Oh, K. Hono, T. Furuhara, T. Maki. Acta Materialia **55**, *15*, 5027 (2007). http://dx.doi.org/10.1016/j.actamat.2007.05.023
[23] B. Kim, C. Celada, D. San Martín, T. Sourmail, P.E.J. Rivera-Diaz-del-Castillo. Acta Materialia **61**, *18*, 6983 (2013). http://dx.doi.org/10.1016/j.actamat.2013.08.012
[24] T. Xu, Z. He, N. lv, X. Han, B. Wang, X. Hou. J. Mater. Sci. **57**, *48*, 22067 (2022). https://doi.org/10.1007/s10853-022-07996-x
[25] A.N. Makovetskii, D.A. Mirzaev, A.A. Mirzoev, K.Yu. Okishev. Vestnik YuUrGU. Seriya „Metallurgiya" **17**, *4*, 38 (2017). (in Russian). https://doi.org/10.14529/met170404
[26] S.V. Vonsovskii. Magnetizm. Nauka, M. (1971). 805 s. (in Russian).
[27] V.I. Petinov. Tech. Phys. **59**, *1*, 6 (2014).
[28] S.P. Gubin, Yu.A. Koksharov, G.B. Khomutov, G.Yu. Yurkov. Russ. Chem. Rev. **74**, *6*, 489 (2005).
[29] J.M.D. Coey. Magnetism and Magnetic Materials. Cambridge University Press, Cambridge (2010). 614 p.
[30] H.-J. Choe, T. Terai, T. Fukuda, T. Kakeshita, S. Yamamoto, M. Yonemura. JMMM **417**, 1 (2016). https://doi.org/10.1016/j.jmmm.2016.05.008
[31] A.I. Ul'yanov, A.A. Chulkina. Phys. Metals. Metallogr. **107**, *5*, 439 (2009).

Translated by M.Shevelev